

Renormalization group evolution of multi-gluon correlators in high energy QCD

A. Dumitru,^{1,2,3} J. Jalilian-Marian,^{2,3} T. Lappi,^{4,5} B. Schenke,⁶ and R. Venugopalan⁶

¹*RIKEN BNL Research Center, Brookhaven National Laboratory, Upton, NY-11973, USA*

²*Department of Natural Sciences, Baruch College, CUNY,
17 Lexington Avenue, New York, NY 10010, USA*

³*The Graduate School and University Center, CUNY, 365 Fifth Avenue, New York, NY 10016, USA*

⁴*Department of Physics, P.O. Box 35, 40014 University of Jyväskylä, Finland*

⁵*Helsinki Institute of Physics, P.O. Box 64, 00014 University of Helsinki, Finland*

⁶*Physics Department, Brookhaven National Laboratory, Upton, NY-11973, USA*

Many-body QCD in leading high energy Regge asymptotics is described by the Balitsky-JIMWLK hierarchy of renormalization group equations for the x evolution of multi-point Wilson line correlators. These correlators are universal and ubiquitous in final states in deeply inelastic scattering and hadronic collisions. For instance, recently measured di-hadron correlations at forward rapidity in deuteron-gold collisions at the Relativistic Heavy Ion Collider (RHIC) are sensitive to four and six point correlators of Wilson lines in the small x color fields of the dense nuclear target. We evaluate these correlators numerically by solving the functional Langevin equation that describes the Balitsky-JIMWLK hierarchy. We compare the results to mean-field Gaussian and large N_c approximations used in previous phenomenological studies. We comment on the implications of our results for quantitative studies of multi-gluon final states in high energy QCD.

PACS numbers: 24.85.+p, 25.75.Gz, 12.38.Lg

I. INTRODUCTION

QCD in high energy Regge asymptotics can be described as a dense many-body system of “wee” gluons and sea quarks. In the infinite momentum frame, gluons with transverse momenta $k_\perp \lesssim Q_s$ saturate phase space maximally, where $Q_s(x)$ is a dynamical saturation scale [1] that grows with decreasing fractions x of the longitudinal momentum of the hadron carried by the gluons. The properties of saturated gluons are described by the Color Glass Condensate (CGC) effective theory [2, 3], where the degrees of freedom are static color sources in the hadron at large x , coupled to the dynamical wee gluon fields at small x . Renormalization group equations, derived from requiring that observables be independent of the separation in x between sources and fields, lead to an infinite hierarchy of evolution equations in x , for n -point Wilson line correlators averaged over dense color fields in the hadron. Given appropriate initial conditions at large x , solutions of this Balitsky-JIMWLK hierarchy [4, 5] allow one to compute a wide range of multi-particle final states in deeply inelastic scattering (DIS) and hadronic collisions.

A prominent example is provided by inclusive DIS structure functions F_2 and F_L , which are proportional to the forward scattering amplitude of a $q\bar{q}$ “dipole” on a nucleus. The forward dipole amplitude (dipole cross section) can be expressed as

$$\sigma_{\text{dip.}}(x, \mathbf{r}_T) = 2 \int d^2 \mathbf{b}_T \times \left\langle 1 - \frac{1}{N_c} \text{Tr} V \left(\mathbf{b}_T + \frac{\mathbf{r}_T}{2} \right) V^\dagger \left(\mathbf{b}_T - \frac{\mathbf{r}_T}{2} \right) \right\rangle, \quad (1)$$

where $\mathbf{r}_T = \mathbf{x}_T - \mathbf{y}_T$ is the transverse size of the dipole, $\mathbf{b}_T = (\mathbf{x}_T + \mathbf{y}_T)/2$ is the impact parameter relative to the

hadron, and the rapidity $Y = \ln(x_0/x)$, where x_0 is the initial scale for small x evolution. The dipole amplitude is the expectation value $D \equiv \langle \hat{D} \rangle$ of the dipole operator

$$\hat{D}(\mathbf{x}_T - \mathbf{y}_T) \equiv \frac{1}{N_c} \text{Tr} V(\mathbf{x}_T) V^\dagger(\mathbf{y}_T) \quad (2)$$

averaged over the color sources of the target evaluated at the rapidity Y . This average obeys the Balitsky-JIMWLK equation that relates its energy dependence to the expectation value of a four-point operator:

$$\frac{d}{dY} D(\mathbf{x}_T - \mathbf{y}_T) = \frac{N_c \alpha_s}{2\pi^2} \int_{\mathbf{z}_T} \frac{(\mathbf{x}_T - \mathbf{y}_T)^2}{(\mathbf{x}_T - \mathbf{z}_T)^2 (\mathbf{z}_T - \mathbf{y}_T)^2} \times \left\langle \hat{D}(\mathbf{x}_T - \mathbf{z}_T) \hat{D}(\mathbf{z}_T - \mathbf{y}_T) - \hat{D}(\mathbf{x}_T - \mathbf{y}_T) \right\rangle. \quad (3)$$

In the large N_c approximation the expectation value of \hat{D}^2 factorizes and the equation becomes a closed one. This is known as the Balitsky-Kovchegov (BK) equation [4, 6]:

$$\frac{d}{dY} D(\mathbf{x}_T - \mathbf{y}_T) = \frac{N_c \alpha_s}{2\pi^2} \int_{\mathbf{z}_T} \frac{(\mathbf{x}_T - \mathbf{y}_T)^2}{(\mathbf{x}_T - \mathbf{z}_T)^2 (\mathbf{z}_T - \mathbf{y}_T)^2} \times [D(\mathbf{x}_T - \mathbf{z}_T) D(\mathbf{z}_T - \mathbf{y}_T) - D(\mathbf{x}_T - \mathbf{y}_T)]. \quad (4)$$

In addition to Eq. (1), this dipole correlator appears in a number of final states in both DIS and hadronic scattering; the BK equation for its energy evolution is widely used in phenomenological applications. The mean field approximation $\langle \hat{D}^2 \rangle \approx \langle \hat{D} \rangle^2$ has been checked by numerical solutions of the JIMWLK equations, and it is seen that it is satisfied to a very good approximation (much better than the $1/N_c^2$ one might expect) [7, 8]. Unless noted otherwise, throughout the paper we define

the saturation scale $Q_s(Y)$ from the expectation value of the dipole operator as $D(r = \sqrt{2}/Q_s) = e^{-1/2}$.

For less inclusive observables, new universal degrees of freedom beyond dipoles are encountered. Examples include small- x di-jet production in e+A DIS [9], quark-antiquark pair production in hadronic collisions [10] and near-side long-range rapidity correlations [11]. Here we focus on n -point functions which appear in forward di-hadron production in light on heavy hadron collisions,

$$\frac{d\sigma^{qA \rightarrow qgX}}{d^3k_1 d^3k_2} \propto \frac{\alpha_s N_c}{2} \int_{\mathbf{x}_T, \bar{\mathbf{x}}_T, \mathbf{y}_T, \bar{\mathbf{y}}_T} e^{-i\mathbf{k}_{T1} \cdot (\mathbf{x}_T - \bar{\mathbf{x}}_T)} e^{-i\mathbf{k}_{T2} \cdot (\mathbf{y}_T - \bar{\mathbf{y}}_T)} \mathcal{F}(\bar{\mathbf{x}}_T - \bar{\mathbf{y}}_T, \mathbf{x}_T - \mathbf{y}_T) \left\langle \hat{Q}(\mathbf{y}_T, \bar{\mathbf{y}}_T, \bar{\mathbf{x}}_T, \mathbf{x}_T) \hat{D}(\mathbf{x}_T, \bar{\mathbf{x}}_T) \right. \\ \left. - \hat{D}(\mathbf{y}_T, \mathbf{x}_T) \hat{D}(\mathbf{x}_T, \bar{\mathbf{z}}_T) - \hat{D}(\mathbf{z}_T, \bar{\mathbf{x}}_T) \hat{D}(\bar{\mathbf{x}}_T, \bar{\mathbf{y}}_T) + \frac{C_F}{N_c} \hat{D}(\mathbf{z}_T, \bar{\mathbf{z}}_T) + \frac{1}{N_c^2} \left(\hat{D}(\mathbf{y}_T, \bar{\mathbf{z}}_T) + \hat{D}(\mathbf{z}_T, \bar{\mathbf{y}}_T) - \hat{D}(\mathbf{y}_T, \bar{\mathbf{y}}_T) \right) \right\rangle, \quad (5)$$

with $\mathbf{z}_T = z\mathbf{x}_T + (1-z)\mathbf{y}_T$ and likewise, $\bar{\mathbf{z}}_T = z\bar{\mathbf{x}}_T + (1-z)\bar{\mathbf{y}}_T$. \mathcal{F} denotes the splitting function for producing a photon off a quark, with the four co-ordinates denoting the transverse spatial co-ordinates of the quark and gluon in the amplitude and conjugate amplitude. The color field dynamics specific to gluon emission are absorbed in the expectation value $\langle \rangle$, which contains a new quadrupole operator,

$$\hat{Q}(\mathbf{x}_T, \mathbf{y}_T, \mathbf{u}_T, \mathbf{v}_T) = \frac{1}{N_c} \text{Tr} V(\mathbf{x}_T) V^\dagger(\mathbf{y}_T) V(\mathbf{u}_T) V^\dagger(\mathbf{v}_T). \quad (6)$$

We denote the expectation value of the quadrupole operator by $Q = \langle \hat{Q} \rangle$. Unlike the $\langle \hat{D}^2 \rangle$ in Eq. (3), it is not reducible to the product of dipoles even in the large N_c and large A approximations and is a novel universal correlator in high energy QCD [9, 13], interesting both from theoretical and phenomenological perspectives.

In this paper, we determine the expectation values of relevant Wilson line correlators for a SU(3) gauge group explicitly numerically. It is known that the evolution of the expectation values of Wilson line correlators can be expressed as a functional Fokker-Planck equation [14], which in turn can be re-expressed as a functional Boltzmann-Langevin equation for the Wilson lines themselves [15],

$$\frac{dV(\mathbf{x}_T)}{dY} = V(\mathbf{x}_T) (it^a) \left\{ \sigma(\mathbf{x}_T)^a + \int_{\mathbf{z}_T} \varepsilon(\mathbf{x}_T, \mathbf{z}_T)_i^{ab} \xi(\mathbf{z}_T)_i^b \right\} \quad (7)$$

where

$$\varepsilon(\mathbf{x}_T, \mathbf{z}_T)_i^{ab} = \left(\frac{\alpha_s}{\pi} \right)^{1/2} \frac{(\mathbf{x}_T - \mathbf{z}_T)_i}{(\mathbf{x}_T - \mathbf{z}_T)^2} [1 - U(\mathbf{x}_T)^\dagger U(\mathbf{z}_T)]^{ab} \quad (8)$$

is the “square root” of the JIMWLK Hamiltonian. Here U ’s are adjoint Wilson lines, which are related to fundamental Wilson lines through the identity, $U_{ab}(\mathbf{x}_T) =$

$p + A \rightarrow h_1 h_2 X$, a process that has been studied recently in deuteron-gold collisions at RHIC. When both hadrons are produced at forward rapidities in the proton/deuteron fragmentation region, the dominant underlying QCD process is the scattering of a large x_1 valence quark from the deuteron off small x_2 partons in the nuclear target, with the emission of a gluon from the valence quark either before or after the collision. This cross-section is expressed as [9, 12],

$2 \text{Tr}(t^a V^\dagger(\mathbf{x}_T) t^b V(\mathbf{x}_T))$. The equation includes a term proportional to a Gaussian white noise ξ satisfying $\langle \xi(\mathbf{x}_T)_i^b \rangle = 0$ and $\langle \xi(\mathbf{x}_T)_i^a \xi(\mathbf{y}_T)_j^b \rangle = \delta^{ab} \delta^{ij} \delta^{(2)}(\mathbf{x}_T - \mathbf{y}_T)$. Finally, there is also a drag term

$$\sigma(\mathbf{x}_T)^a = -i \frac{\alpha_s}{2\pi^2} \int_{\mathbf{z}_T} \frac{1}{(\mathbf{x}_T - \mathbf{z}_T)^2} \text{Tr} [T^a U(\mathbf{x}_T)^\dagger U(\mathbf{z}_T)], \quad (9)$$

where T^a is a generator of the adjoint representation.

II. NUMERICAL METHOD

As alluded to previously, numerical solutions of the Boltzmann-Langevin hierarchy were obtained for fixed coupling [7] and used to study the factorization of dipole correlators. Apart from the running coupling, we use the numerical method of ref. [7] for solving the JIMWLK equation. Several running coupling prescriptions have been suggested in the literature [16]; in this paper, as in [17], we will assume that the coupling constant runs as a function of the “daughter” dipole size $r = |\mathbf{x}_T - \mathbf{z}_T|$. The Landau pole is regulated by taking

$$\alpha_s(r) = \frac{4\pi}{\beta \ln \left\{ \left[\left(\frac{\mu_0^2}{\Lambda^2} \right)^{\frac{1}{c}} + \left(\frac{4}{r^2 \Lambda^2} \right)^{\frac{1}{c}} \right]^c \right\}}, \quad (10)$$

with a parameter c which regulates the sharpness of the cutoff. The scale Λ in the coupling is parametrically of the order of Λ_{QCD} , but the exact value that should be used is scheme dependent.

The initial conditions are those of the McLerran-Venugopalan (MV) model [18]; one has for the initial rapidity $Y = 0$, $V(\mathbf{x}_T) = \prod_{k=1}^{N_y} \exp(-i \frac{g \rho_k(\mathbf{x}_T)}{\sqrt{2}})$ with $\langle \rho_k^a(\mathbf{x}_T) \rho_l^b(\mathbf{y}_T) \rangle = g^2 \mu^2 \delta^{(2)}(\mathbf{x}_T - \mathbf{y}_T) \delta^{ab} \delta^{kl} / N_y$, with the

indices $k, l = 1 \dots N_y$ representing a discretized longitudinal coordinate, taking care of the finite extension of the source in the x^- direction. The normalization is chosen such that $\sum_{k,l} \langle \rho_k^a(\mathbf{x}_T) \rho_l^b(\mathbf{y}_T) \rangle = g^2 \mu^2 \delta^{(2)}(\mathbf{x}_T - \mathbf{y}_T) \delta^{ab}$. Given the numerical implementation of this initial condition [19] for the V 's, using a longitudinal resolution of $N_y = 100$, one can then solve Eq. (7) on a 2-D lattice. The Poisson equation is solved by leaving out the zero transverse momentum mode. This procedure corresponds to an infrared cutoff given by the size of the system. The calculation is performed on a regular square lattice of N_T^2 sites with periodic boundary conditions. Its volume is $(N_T a)^2$ where a is the lattice spacing. In the calculations presented we use $N_T = 512$ unless otherwise stated, and $\delta s = 0.00026$, $g^2 \mu a = 0.109375$. The parameters controlling the running coupling are taken as $c = 0.2$, $\Lambda = 0.0536 g^2 \mu$, and $\mu_0 = 2.5 \Lambda$. These parameters are chosen to be close to the phenomenologically realistic range for the speed of evolution as observed in fits to $F_2(x, Q^2)$ data, but have not been adjusted to give a best possible fit.

III. NAIVE LARGE N_c APPROXIMATION

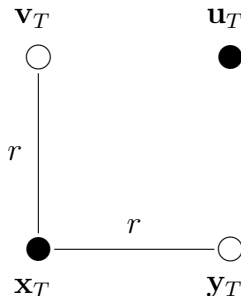


FIG. 1: Square arrangement of the coordinates in Eq. (6). The filled circles represent Wilson lines and the open ones conjugates.

We will first present results for the expectation value of the quadrupole correlator Q . Since this correlator is a function of four independent two dimensional spatial vectors, we will for simplicity study its properties for two specific spatial configurations, one of which is the square configuration $Q_{\square}(r)$, which has the four coordinates arranged in a square of size $r = |\mathbf{x}_T - \mathbf{y}_T|$ as shown in Fig. 1. The other is a simple line configuration $Q_{\parallel}(r)$, where $\mathbf{u}_T = \mathbf{x}_T$, $\mathbf{v}_T = \mathbf{y}_T$ and $r = |\mathbf{x}_T - \mathbf{y}_T| = |\mathbf{u}_T - \mathbf{v}_T|$. The expectation values of all correlators are computed by averaging over all positions on the 2D lattice and 20 different initial configurations.

A “naive” large N_c approximation for Eq. (6) considered previously in phenomenological studies is

$$Q(\mathbf{x}_T, \mathbf{y}_T, \mathbf{u}_T, \mathbf{v}_T) \underset{N_c \rightarrow \infty}{\approx} \frac{1}{2} (D(\mathbf{x}_T, \mathbf{y}_T) D(\mathbf{u}_T, \mathbf{v}_T) + D(\mathbf{x}_T, \mathbf{v}_T) D(\mathbf{u}_T, \mathbf{y}_T)) \quad (11)$$

On inspection, it is apparent that this approximation is problematic because it does not reduce to all the right “coincidence limits”; taking $\mathbf{u}_T = \mathbf{v}_T$ one has $Q(\mathbf{x}_T, \mathbf{y}_T, \mathbf{u}_T, \mathbf{u}_T) = D(\mathbf{x}_T, \mathbf{y}_T)$, but the r.h.s. of Eq. (11) reduces to $\frac{1}{2} (D(\mathbf{x}_T, \mathbf{y}_T) + D(\mathbf{x}_T, \mathbf{u}_T) D(\mathbf{u}_T, \mathbf{y}_T))$ instead. Plots of the JIMWLK solution for the line and square configurations respectively compared to the “naive” approximation

$$Q_{\parallel}^{\text{naive}}(r) = Q_{\square(r)}^{\text{naive}} = D(r)^2 \quad (12)$$

are shown in Fig. 2. It is apparent that the approximation fails even for the initial condition at $Y = 0$, a result that is not ameliorated by the JIMWLK RG evolution. The disagreement between the JIMWLK and approximate results is greater for the line configuration than the square configuration.

IV. GAUSSIAN APPROXIMATION

The fact that the expectation value of the quadrupole correlator does not factorize in the naive way of Eq. (11) was pointed out in [20] and is seen explicitly already in the MV model that specifies the initial conditions¹. We will in this paper compare the JIMWLK result for Q to a “Gaussian” approximation [22, 23] (also referred to as Gaussian Truncation [3, 8]). This is obtained by assuming that the correlators of the color charges are Gaussian variables even after JIMWLK evolution, and therefore all the higher point functions can be expressed in terms of a single two point correlation function, $-\ln(D(\mathbf{x}_T - \mathbf{y}_T)) \equiv \frac{C_F}{2} \Gamma(\mathbf{x}_T - \mathbf{y}_T)$ in the notations of ref. [9]. We obtain this two point function from our solution of the JIMWLK equation. However, as shown in ref. [8], using the solution of the BK equation for the two point function would also be a very good approximation. The Gaussian approximation has also been motivated formally at asymptotically small x in ref. [24]. Thus in the Gaussian approximation the higher point functions are related to the two point function similarly as in the MV model. For the specific case of the quadrupole Q the explicit expression has been derived in ref. [9].

For the square and line configurations we consider here, the cumbersome general Gaussian expression for

¹ We leave the study of quartic contributions [21] to the MV action for future study.

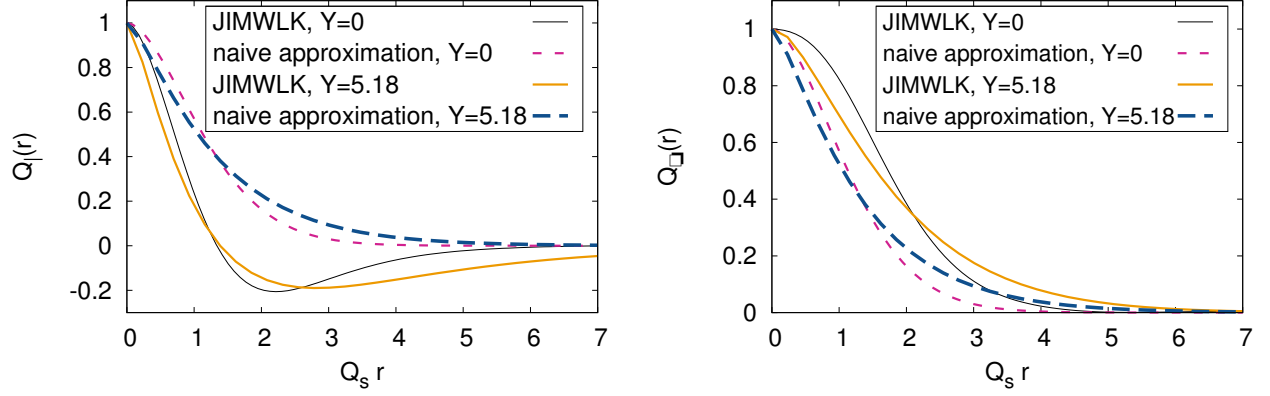


FIG. 2: The four point function Q for coordinates in the line configuration (left) and the square configuration (right) for the initial condition ($Y = 0$) and after evolution ($Y = 5.2$). The JIMWLK quadrupole expectation value (solid lines) is compared to the naive approximation in Eq. (12) (dashed lines).

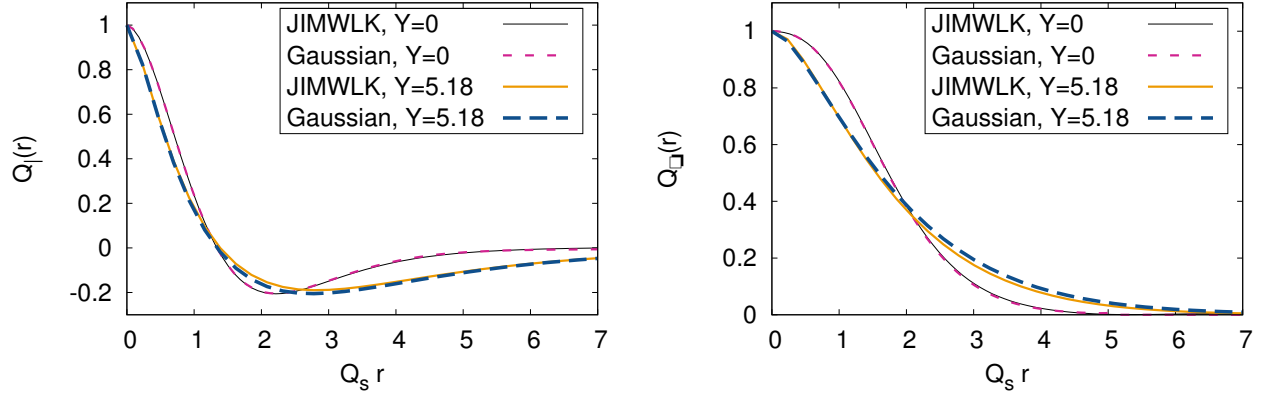


FIG. 3: The four point function Q for coordinates in the line configuration (left) and the square configuration (right) for the initial condition ($Y = 0$) and after evolution ($Y = 5.2$). The JIMWLK quadrupole expectation value (solid lines) is compared to the Gaussian approximation (dashed lines) Eqs. (13), (14) .

the quadrupole correlator simplifies greatly and we find,

$$Q_l(r) \underset{N_c \ll \infty}{\approx} \frac{N_c + 1}{2} (D(r))^{2 \frac{N_c + 2}{N_c + 1}} - \frac{N_c - 1}{2} (D(r))^{2 \frac{N_c - 2}{N_c - 1}} \quad (13)$$

$$Q_s(r) \underset{N_c \ll \infty}{\approx} (D(r))^2 \left[\frac{N_c + 1}{2} \left(\frac{D(r)}{D(\sqrt{2}r)} \right)^{\frac{2}{N_c + 1}} - \frac{N_c - 1}{2} \left(\frac{D(\sqrt{2}r)}{D(r)} \right)^{\frac{2}{N_c - 1}} \right]. \quad (14)$$

In Fig. 3, the numerical results from the solution of the JIMWLK RG equation for the quadrupole (in the line and square configurations) are compared to this Gaussian approximation. When computing the Gaussian approximation, we chose to only calculate the averages in D from contributions aligned with the square or the line configuration, respectively. While the agreement of Q with its Gaussian approximation for the initial condition $Y = 0$ is

required by definition (because one has MV initial conditions in both cases), the agreement of the JIMWLK simulation with the evolved Gaussian approximation is remarkably good. This suggests that the computations in ref. [22, 25] that rely on this approximation may, at least in this aspect, be robust.

If one takes the large N_c limit of the expressions in Eqs. (13) and (14), one finds that

$$Q_l(r) \underset{N_c \rightarrow \infty}{=} D^2(r) [1 + 2 \ln(D(r))] , \quad (15)$$

$$Q_s(r) \underset{N_c \rightarrow \infty}{=} D^2(r) \left[1 + 2 \ln \left(\frac{D(r)}{D(\sqrt{2}r)} \right) \right] . \quad (16)$$

The JIMWLK result compared to this particular large N_c approximation is shown in Fig. 4. The agreement of the large N_c Gaussian approximation with the JIMWLK result is quite good for Q_s , especially for the initial condition; it is less so for Q_l . In the latter case, the agreement for small rQ_s is good, with discrepancies showing up for $rQ_s \gtrsim 1$. We note that the difference between the “naive”

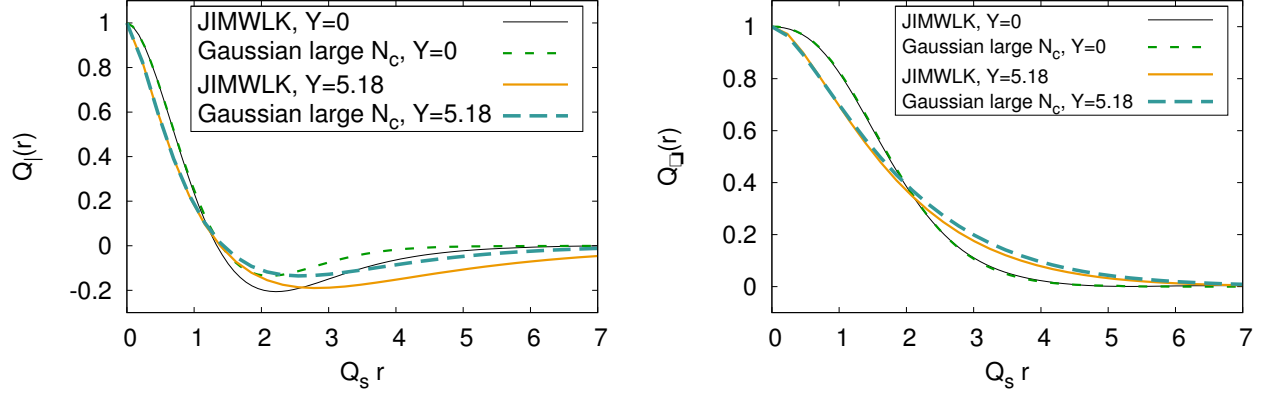


FIG. 4: The four point function Q for coordinates in the line configuration (left) and the square configuration (right) for the initial condition ($Y = 0$) and after evolution ($Y = 5.2$). The JIMWLK quadrupole expectation value (solid lines) is compared to the large N_c limit of the Gaussian approximation, Eqs. (15), (16) (dashed lines).

approximation (12) and this Gaussian large N_c approximation (13), (14) is in the additional logarithmic term in the latter. In the case of the line configuration, this provides some insight into the discrepancy of the naive approximation with the result from JIMWLK evolution. The latter is not constrained to be greater than zero, while the former is. The additional logarithmic term relaxes this constraint because it can change the sign of the result.

V. GEOMETRIC SCALING OF THE QUADRUPOLE

We now turn from this comparison of the quadrupole expectation value to study aspects of its evolution determined from the solution of the JIMWLK equation. The RG evolution of the quadrupole has been studied previously [13, 26] in the large N_c limit of Mueller's dipole model [27]. In particular, it has been argued very recently in ref. [26] that quadrupole evolution should demonstrate geometrical scaling [28].

Our results are shown in Fig. 5. On the left we plot Q_\square as a function of rQ_s . We observe that after initial transient behavior the amplitude Q_\square settles on a shape that is a universal function of rQ_s . Thus for a given x and Q^2 probed in a process, the quadrupole amplitude depends only on the combination proportional to $Q_s(x)^2/Q^2$ thereby demonstrating geometrical scaling for this quantity.

We previously defined the usual saturation scale Q_s through the dipole operator as $D(r = \sqrt{2}/Q_s) = e^{-1/2}$. One can analogously characterize the evolution of the quadrupole by introducing “quadrupole saturation scales” corresponding to the square and line coordinate arrangements. We define these as $Q_{|\square} (r = \sqrt{2}/Q_{|\square}) = e^{-1/2}$. On the right of Fig. 5 we show the evolution speeds $\lambda = d \ln Q_s^2 / dY$ of these different saturation scales, λ for

the dipole and $\lambda^{QL}, \lambda^{QS}$ for the quadrupole in the line and square configurations respectively. The plot shows that initially the quadrupole evolves more rapidly than the dipole. After about 6 units in rapidity, the evolution reaches a universal geometrical scaling regime and the λ parameters settle to a common value.

VI. SIX POINT FUNCTION AND DIHADRON CORRELATIONS

Let us now return to the expression we had in Eq. (5) for forward di-hadron production in hadronic collisions. Experiments at RHIC for deuteron-gold scattering at high energies have shown that the away-side peak in di-hadron correlations is significantly broadened for central collisions at forward rapidities [29] as predicted in the CGC framework [12] and confirmed in more detailed analyses [30]. However, these analyses relied on factorization assumptions that, as we have seen, are not justified because the quadrupole correlator is not simply factorizable. It is not the quadrupole correlator that appears directly in Eq. (5), so we shall now consider the expression

$$S_6(\mathbf{x}_T, \mathbf{y}_T, \mathbf{u}_T, \mathbf{v}_T) = \frac{N_c^2}{N_c^2 - 1} \times \left\langle \hat{Q}(\mathbf{x}_T, \mathbf{y}_T, \mathbf{u}_T, \mathbf{v}_T) \hat{D}(\mathbf{v}_T, \mathbf{u}_T) - \frac{1}{N_c^2} \hat{D}(\mathbf{x}_T, \mathbf{y}_T) \right\rangle, \quad (17)$$

corresponding to the first and last terms in the brackets in Eq. (5). The JIMWLK evolution equation for this quantity was derived recently [20]. As for the quadrupole correlator, we would like to compare numerical results for S_6 to a Gaussian approximation. The latter, however, would strictly require that one compute the product $\langle \hat{Q} \hat{D} \rangle$ in this approximation. Since results for this quantity are not at present available, we will assume that

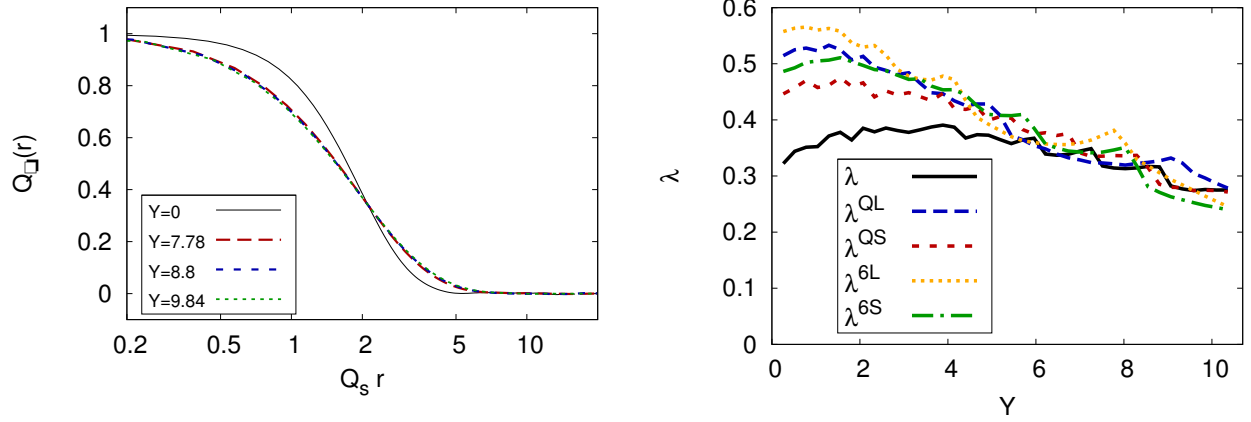


FIG. 5: Left: The JIMWLK quadrupole amplitude Q_\square for the square configuration versus the scaling variable $Q_s r$ (on a logarithmic axis). After initial transient behavior, the amplitude settles to a universal curve (for $Y \geq 7.8$) which depends on $Q_s r$ alone. Right: The evolution speed $\lambda = d \ln Q_s^2 / dY$ extracted from the dipole amplitude D , the quadrupole amplitude in the two spatial configurations (line and square, $\lambda^{QL}, \lambda^{QS}$) and the six point function S_6 , also in the two spatial configurations ($\lambda^{6L}, \lambda^{6S}$).

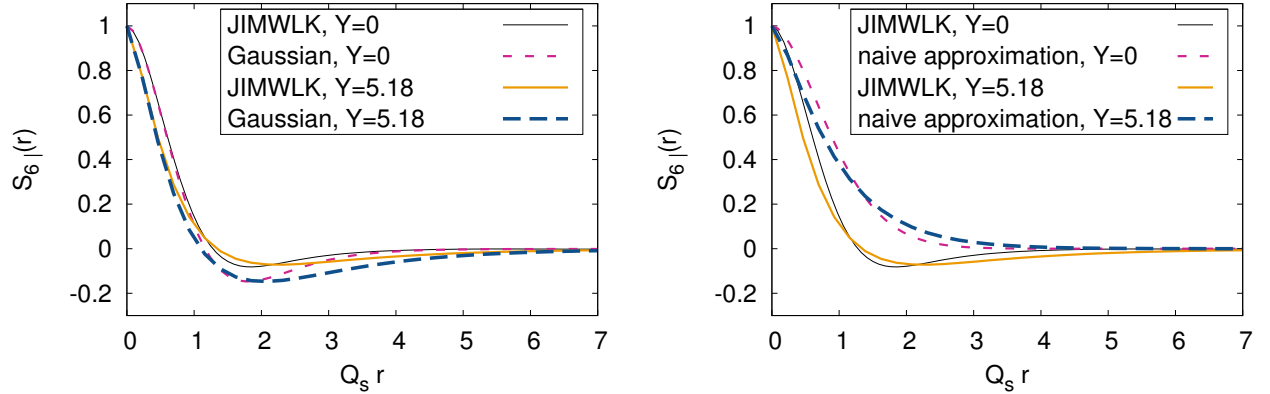


FIG. 6: Left: The JIMWLK result for S_6 (see text) plotted for the line configuration compared to the Gaussian approximation for S_6 . Right: The JIMWLK result compared to a naive large N_c result.

$\langle \hat{Q} \hat{D} \rangle \approx \langle \hat{Q} \rangle \langle \hat{D} \rangle$ and compare the $N_c = 3$ Gaussian approximation for $\langle \hat{Q} \rangle \langle \hat{D} \rangle$ to the numerical JIMWLK results for S_6 . Figure 6 (left) shows the result for the line configuration for S_6 . We observe that the agreement of the JIMWLK and approximate results is quite good for $rQ_s \ll 1$ or $rQ_s \gg 1$, but that there are noticeable deviations in the region $1 \lesssim rQ_s \lesssim 3$. Due to the good agreement of Q with the Gaussian approximation from Eqs. (13), (14) shown above, we interpret these deviations for S_6 as $\mathcal{O}(1/N_c)$ corrections to $\langle \hat{Q} \hat{D} \rangle \approx \langle \hat{Q} \rangle \langle \hat{D} \rangle$. For the square configuration of S_6 (not shown) the deviations are much less, as was the case for the quadrupole. In Fig. 6 (right), we plot the JIMWLK results against the “naive” large N_c approximation $S_{6|}(r) \approx S_{6\Box}(r) \approx D(r)^3$ that has previously been considered in the literature. Once again the deviations are large, suggesting that this approximation is not tenable. We characterize the six-point function by the saturation scales $Q_s^{6|\Box}$, defined by $S_{6|\Box}(r = \sqrt{2}/Q_s^{6|\Box}) = e^{-1/2}$. The corresponding evolu-

tion speeds are also shown in Fig. 5.

As a final result, we present a visualization of JIMWLK evolution that demonstrates the role of fluctuations. In high energy QCD, fluctuations from event-to-event can occur because of fluctuations in the impact parameter positions of gluons, in their position in rapidity, and in the fluctuations in the number of gluons [31]. All of these fluctuations are captured in the numerical simulations of the JIMWLK hierarchy. These results are shown in Fig. 7, which shows the fluctuations of the Wilson lines in the transverse plane at different rapidities. The decreasing of the correlation length $\sim 1/Q_s$ with energy is clearly visible.

To summarize, we have in this work performed simulations of the running coupling SU(3) JIMWLK equation that describes the behavior of expectation values of Wilson line correlators in high energy QCD. We have presented first results for the evolution of specific higher n -point functions which are related to experimental observ-

FIG. 7: (animated online, requires Acrobat reader) Correlation $1/N_c \langle V^\dagger(0,0)V(x,y) \rangle$ between the center position $(0,0)$ and the point (x,y) for three different rapidities Y . This illustrates the degree of fluctuations and shows how the correlation length decreases dynamically with increasing Y . The first image can be animated to show the evolution with rapidity.

ables in DIS and in p+p, p+A collisions. In particular, we find that the “quadrupole” correlator can be approximated quite well by a careful Gaussian approximation for $N_c = 3$. The $N_c \rightarrow \infty$ Gaussian approximation is accurate at short distances, $rQ_s \lesssim 1$, but may display more significant relative deviations in the saturation regime, $rQ_s \gtrsim 1$. We have also provided evidence for travelling wave solutions and geometric scaling for the quadrupole.

Acknowledgements

Discussions with G. Beuf, F. Dominguez, F. Gelis, E. Iancu, A. H. Mueller, K. Rummukainen, H. Weigert, D. Triantofyllopoulos, B.-W. Xiao and F. Yuan are grate-

fully acknowledged. T.L. has been supported by the Academy of Finland, projects 126604 and 141555 and by computing resources from CSC – IT Center for Science in Espoo, Finland. He thanks the Nuclear Theory Group at BNL for its hospitality during the early stages of this work. B.P.S. and R.V. are supported by US Department of Energy under DOE Contract No. DE-AC02-98CH10886. A.D. and J.J.-M. acknowledge support by the DOE Office of Nuclear Physics through Grant No. DE-FG02-09ER41620 and from The City University of New York through the PSC-CUNY Research Award Program, grants 63382-0041 (A.D.) and 63404-0041 (J.J.-M.). We acknowledge support from the “Lab Directed Research and Development” grant LDRD 10-043 (Brookhaven National Laboratory),

-
- [1] L. V. Gribov, E. M. Levin and M. G. Ryskin *Phys. Rept.* **100** (1983) 1; A. H. Mueller and J.-w. Qiu *Nucl. Phys.* **B268** (1986) 427.
 - [2] E. Iancu and R. Venugopalan in *Quark gluon plasma* (R. Hwa and X. N. Wang, eds.). World Scientific, 2003. [arXiv:hep-ph/0303204](#); F. Gelis, E. Iancu, J. Jalilian-Marian and R. Venugopalan *Ann.Rev.Nucl.Part.Sci.* **60** (2010) 463 [[arXiv:1002.0333 \[hep-ph\]](#)].
 - [3] H. Weigert *Prog. Part. Nucl. Phys.* **55** (2005) 461 [[arXiv:hep-ph/0501087](#)].
 - [4] I. Balitsky *Nucl. Phys.* **B463** (1996) 99 [[arXiv:hep-ph/9509348](#)].
 - [5] J. Jalilian-Marian, A. Kovner, A. Leonidov and H. Weigert *Nucl. Phys.* **B504** (1997) 415 [[arXiv:hep-ph/9701284](#)]; J. Jalilian-Marian, A. Kovner, A. Leonidov and H. Weigert *Phys. Rev.* **D59** (1999) 014014 [[arXiv:hep-ph/9706377](#)]; E. Iancu, A. Leonidov and L. D. McLerran *Nucl. Phys.* **A692** (2001) 583 [[arXiv:hep-ph/0011241](#)]; E. Ferreira, E. Iancu, A. Leonidov and L. McLerran *Nucl. Phys.* **A703** (2002) 489 [[arXiv:hep-ph/0109115](#)]; A. H. Mueller *Phys. Lett.* **B523** (2001) 243 [[arXiv:hep-ph/0110169](#)].
 - [6] Y. V. Kovchegov *Phys. Rev.* **D60** (1999) 034008 [[arXiv:hep-ph/9901281](#)].
 - [7] K. Rummukainen and H. Weigert *Nucl. Phys.* **A739** (2004) 183 [[arXiv:hep-ph/0309306](#)].
 - [8] Y. V. Kovchegov, J. Kuokkanen, K. Rummukainen and H. Weigert *Nucl. Phys.* **A823** (2009) 47 [[arXiv:0812.3238 \[hep-ph\]](#)].
 - [9] F. Dominguez, C. Marquet, B.-W. Xiao and F. Yuan *Phys.Rev.* **D83** (2011) 105005 [[arXiv:1101.0715 \[hep-ph\]](#)].
 - [10] J. P. Blaizot, F. Gelis and R. Venugopalan *Nucl. Phys.* **A743** (2004) 57 [[arXiv:hep-ph/0402257](#)].
 - [11] A. Dumitru and J. Jalilian-Marian *Phys. Rev.* **D81** (2010) 094015 [[arXiv:1001.4820 \[hep-ph\]](#)].

- [12] C. Marquet *Nucl. Phys.* **A796** (2007) 41 [arXiv:0708.0231 [hep-ph]].
- [13] J. Jalilian-Marian and Y. V. Kovchegov *Phys. Rev.* **D70** (2004) 114017 [arXiv:hep-ph/0405266].
- [14] H. Weigert *Nucl. Phys.* **A703** (2002) 823 [arXiv:hep-ph/0004044].
- [15] J.-P. Blaizot, E. Iancu and H. Weigert *Nucl. Phys.* **A713** (2003) 441 [arXiv:hep-ph/0206279].
- [16] I. Balitsky and G. A. Chirilli *Phys.Rev.* **D77** (2008) 014019 [arXiv:0710.4330 [hep-ph]]; Y. V. Kovchegov and H. Weigert *Nucl. Phys.* **A784** (2007) 188 [arXiv:hep-ph/0609090].
- [17] T. Lappi arXiv:1105.5511 [hep-ph].
- [18] L. D. McLerran and R. Venugopalan *Phys. Rev.* **D49** (1994) 2233 [arXiv:hep-ph/9309289]; L. D. McLerran and R. Venugopalan *Phys. Rev.* **D49** (1994) 3352 [arXiv:hep-ph/9311205]; L. D. McLerran and R. Venugopalan *Phys. Rev.* **D50** (1994) 2225 [arXiv:hep-ph/9402335].
- [19] T. Lappi *Eur. Phys. J.* **C55** (2008) 285 [arXiv:0711.3039 [hep-ph]].
- [20] A. Dumitru and J. Jalilian-Marian *Phys.Rev.* **D82** (2010) 074023 [arXiv:1008.0480 [hep-ph]].
- [21] A. Dumitru, J. Jalilian-Marian and E. Petreska *Phys.Rev.* **D84** (2011) 014018 [arXiv:1105.4155 [hep-ph]].
- [22] H. Fujii, F. Gelis and R. Venugopalan *Nucl. Phys.* **A780** (2006) 146 [arXiv:hep-ph/0603099].
- [23] C. Marquet and H. Weigert *Nucl.Phys.* **A843** (2010) 68 [arXiv:1003.0813 [hep-ph]].
- [24] E. Iancu, K. Itakura and L. McLerran *Nucl. Phys.* **A724** (2003) 181 [arXiv:hep-ph/0212123].
- [25] K. Dusling, F. Gelis, T. Lappi and R. Venugopalan *Nucl. Phys.* **A836** (2010) 159 [arXiv:0911.2720 [hep-ph]].
- [26] F. Dominguez, A. Mueller, S. Munier and B.-W. Xiao arXiv:1108.1752 [hep-ph].
- [27] A. H. Mueller *Nucl. Phys.* **B415** (1994) 373.
- [28] A. M. Stasto, K. J. Golec-Biernat and J. Kwiecinski *Phys. Rev. Lett.* **86** (2001) 596 [arXiv:hep-ph/0007192]; E. Iancu, K. Itakura and L. McLerran *Nucl. Phys.* **A708** (2002) 327 [arXiv:hep-ph/0203137]; A. H. Mueller and D. N. Triantafyllopoulos *Nucl. Phys.* **B640** (2002) 331 [arXiv:hep-ph/0205167].
- [29] PHENIX collaboration, A. Adare *et. al.* arXiv:1105.5112 [nucl-ex]; E. Braidot arXiv:1102.0931 [nucl-ex].
- [30] J. L. Albacete and C. Marquet *Phys.Rev.Lett.* **105** (2010) 162301 [arXiv:1005.4065 [hep-ph]]; K. Tuchin *Phys.Lett.* **B686** (2010) 29 [arXiv:0911.4964 [hep-ph]].
- [31] H. I. Miettinen and J. Pumplin *Phys.Rev.* **D18** (1978) 1696.